Available online at www.sciencedirect.com
ScienceDirect
Tetrahedron
Tetrahedron 63 (2007) 7086–7096

Peripheral aryl-substituted pyrrole fluorophores for glassy blue-light-emitting diodes

Wen-Jang Kuo,[a,*] Ying-Hsiao Chen,[b] Ru-Jong Jeng,[b,*] Li-Hsin Chan,[c] Wen-Peng Lin[a] and Zhe-Ming Yang[a]

[a]*Department of Applied Chemistry, National University of Kaohsiung, Kaohsiung 811, Taiwan, ROC*
[b]*Department of Chemical Engineering, National Chung Hsing University, Taichung 402, Taiwan, ROC*
[c]*Department of Materials Science and Engineering, I-Shou University, Kaohsiung 840, Taiwan, ROC*

Received 26 March 2007; revised 30 April 2007; accepted 1 May 2007
Available online 13 May 2007

Abstract—In this work, a series of aryl-substituted pyrrole analogues were synthesized. These pyrrole analogues emit violet to blue light. Fluorescence and amorphous glassy properties of these pyrrole analogues were induced by manipulating the peripheral aryl groups. These crowded peripheral aryl groups would effectively prevent the fluorophores from aggregation, resulting in higher quantum efficiency and a stable emission spectrum in the solid state. One of the aryl-substituted pyrrole analogues, namely NPANPy can be used as hole-transporting material or hole-transporting/emitting material. The devices would emit blue light when the fluorophore NPANPy acts as the hole-transporting/emitting material. Their CIE coordinate is around (0.16, 0.14), whereas the maximum brightness can reach 4300–5000 cd m^{-2}. Apart from that, when the fluorophore was used only as the hole-transporting material, better device performances, especially in low current density, were found, as compared with the standard device.

1. Introduction

Since the discovery of small molecule-based and polymer-based organic electroluminescence (OEL) devices by Tang's[1] and Holmes' groups,[2] there have been intense research activities in organic EL devices. Major challenges remain, however, including the need to significantly improve the performance and durability of blue, green, red, and white OLEDs for displays and lighting. Blue emitters for organic EL devices remain the most sought-after materials.[3] By modification of the molecular structures, the color and performance can be manipulated.[4] From the structural aspect, molecules with asymmetric and nonplanar structure can be readily processed into amorphous films by either spin-coating or vacuum deposition.[5] Complete amorphous morphology of films can effectively prevent the formation of aggregates, excimers, and exciplexes, which would result in higher quantum efficiency and a stable emission spectrum. Some starburst and dendron-type conjugated molecules have been proven to be effective molecular construction blocks to inhibit the formation of molecular aggregation or π–π stacking in the solid state.[6] In addition to improving the quantum efficiency, film-forming properties and their temporal stability are prerequisites for the performance and longevity of devices.[7] Amorphous materials possessing high glass transition temperatures (T_g) would be beneficial for forming glasses and avoiding crystal formation which leads to grain boundary problems. By introducing sterically crowded substituents, such as tetraphenylmethyl[8] or tetraphenylsilyl moieties[9] into fluorophores, the molecular self-aggregation would be inhibited in the film state.[6a,10] Such bulky structures can render these compounds amorphous in nature and make it difficult for them to pack into detrimental aggregates in the film state.[11]

In this work, nitrogen-containing cyclic π-electron system, *pyrrole* was used as a novel fluorescent platform. To induce the fluorescent characteristics and prevent aggregation, several aryl groups were grafted onto the pyrrole platform at 2-, 3-, 4-, and 5-position. In order to investigate the fluorescent characteristics affected by the crowded steric effect of the aryl substituents, a variety of aryl-substituted pyrrole fluorophores were synthesized. Some pyrrole fluorophores would be anticipated to exhibit amorphous solid behavior due to the presence of peripheral aryl-substituted moieties, and consequently enhance the luminance efficiency. In order to evaluate the practicality of these fluorophores, double-layer and triple-layer EL devices using these pyrrole-containing compounds as hole-transporting layer and emitting layer, and tris(8-quinolinolato)-aluminum (Alq_3)[12] or 1,3,5-tris(*N*-phenylbenzimidazol-2-yl)benzene (TPBI)[13] as electron-transporting layer were fabricated.

* Corresponding authors. E-mail addresses: wjkuo@nuk.edu.tw; rjjeng@dragon.nchu.edu.tw

0040–4020/$ - see front matter © 2007 Elsevier Ltd. All rights reserved.
doi:10.1016/j.tet.2007.05.032

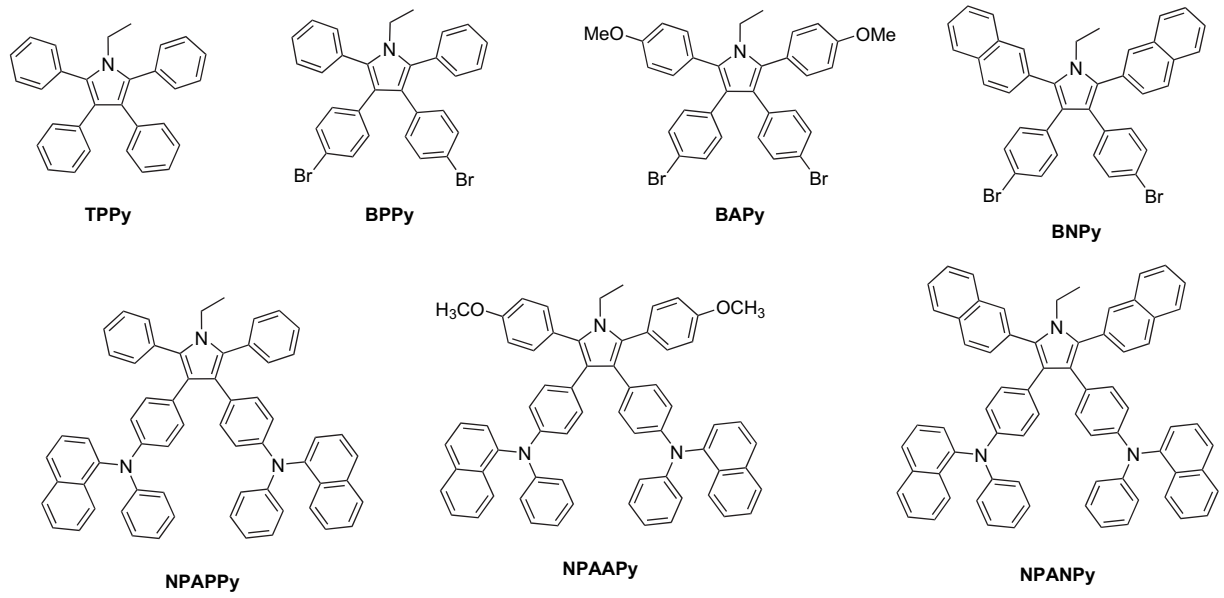

Chart 1. Chemical structures of the pyrrole-containing fluorophores.

2. Results and discussion

2.1. Synthesis and characterization of the aryl-substituted pyrroles

Chart 1 shows the chemical structures of the aryl-substituted pyrrole fluorophores. Suzuki-coupling reaction might be employed in the synthesis of symmetric tetraarylpyrroles. However, it not only failed to give asymmetric aryl-substituted compounds, but generated several side products as well. In order to effectively synthesize symmetric aryl-substituted pyrroles, [2+2+1] cycloaddition reaction was utilized in this work. In addition, Paal–Knorr condensation reaction, which is an effective route to prepare symmetric and asymmetric aryl-substituted pyrrole derivatives was also employed. Scheme 1 shows the synthetic route to the aryl-substituted pyrrole derivatives. Under iodine and sodium methoxide, the deoxybenzoin analogues were oxidatively dimerized first into symmetric or asymmetric tetraaryl-substituted buta-1,4-dione. The pyrrole ring was subsequently formed with the addition of ammonium acetate via the Paal–Knorr condensation reaction. As a result, the aryl-substituted pyrrole analogues with active N–H were obtained. These pyrroles exhibit strong fluorescent quench in the solid state.[14] After further ethylation, solid state fluorescence was found for the pyrrole fluorophores.

2.2. Photophysical properties and energy level

Figure 1 shows the absorption and fluorescence spectra of these pyrrole fluorophores. The UV spectra show similar absorptions around 286 nm caused by the π–π^* excitation of these pyrrole fluorophores. Large bathochromic shift in emission wavelength was found in the emission spectra. As compared to model compound TPPy (Chart 1), the maximum emission wavelengths of the fluorophores BPPy, BAPy, and BNPy (Chart 1) were shifted to 400, 410, and 420 nm, respectively. Obviously, the maximum emission wavelength of the fluorophores was affected by the peripheral aryl groups. By extending the conjugation length of the peripheral aryl groups, i.e., introducing heteroatom functionalized-aryl groups or naphthyl group, the maximum emission wavelength of the pyrrole fluorophores would be red-shifted. These pyrrole fluorophores in solid state exhibit stronger fluorescence intensities than those in dichloromethane solution as shown in the inset photo of Figure 1. This phenomenon differs from many organic fluorophores. They exhibit high fluorescent quantum yields in solution, but the fluorescence is usually quenched in highly concentrated solution or in the solid films because of the existence of more nonradiative decay channels associated with aggregates, excimers, exciplexes, and impurities in the solid state.[15]

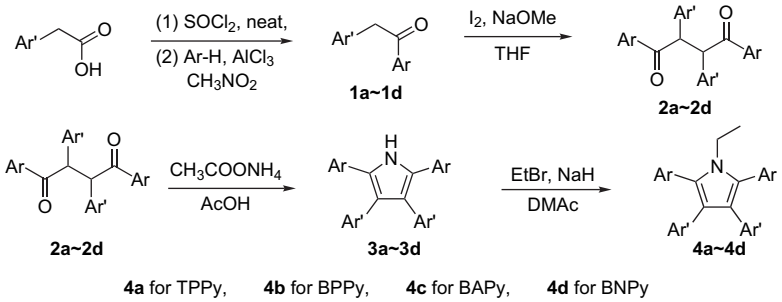

Scheme 1. Synthesis of aryl-substituted pyrrole fluorophores.

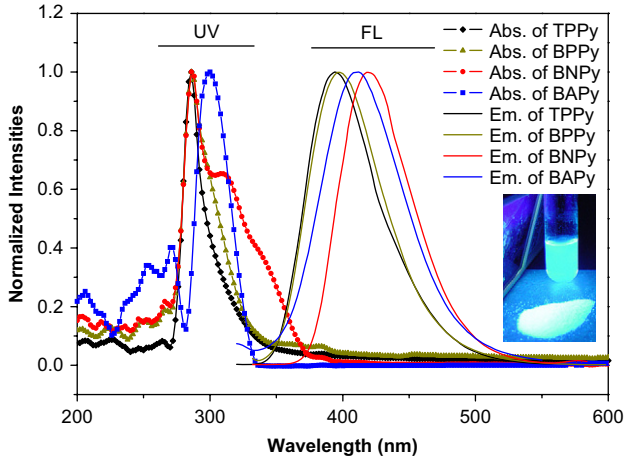

Figure 1. Normalized absorption (dotted line) and fluorescence spectra (solid line) of pyrrole fluorophores in dichloromethane solution. Inset: photo of the fluorophore BPPy luminescence in dichloromethane and solid powder.

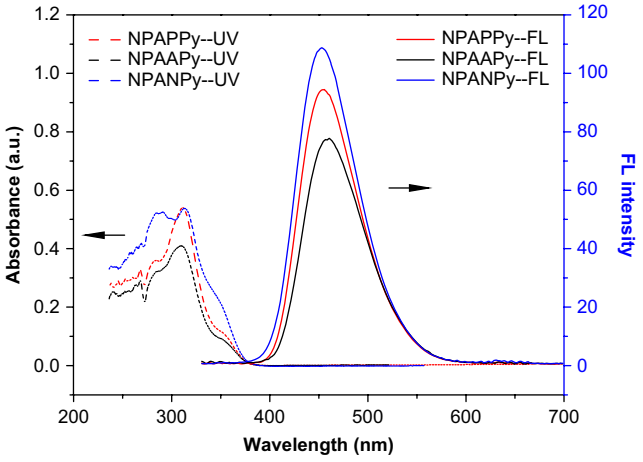

Figure 2. Absorption (dotted line) and fluorescence spectra (solid line) of the amino-pyrrole fluorophores in dichloromethane solution.

The above-mentioned pyrrole fluorophores emitted violet-blue to blue light. To shift color of the emission light to deep blue, the conjugation length would be elongated by introducing arylamino group onto fluorophores. Pd-catalyzed aromatic amination reactions are commonly employed in the synthesis of triarylamines.[16] Scheme 2 shows the synthesis of the pyrrole-based arylamines, NPAPPy, NPAAPy, and NPANPy. After amination, these aminated pyrrole fluorophores bathochromically shifted the emitting light to 450 nm, which was a deep blue hue. Figure 2 shows absorption and emission spectra of the aminated fluorophores in the same concentration. It is interesting that variations of the peripheral aromatic substituents shifted the maximum absorption wavelength slightly but were capable of enhancing their emission intensities in the same concentration (1×10^{-5} M) extensively. This fact may be attributed to the effect of the crowded peripheral aryl groups at 2- and 5-position, in addition to the strong delocalization between the arylamino group and pyrrole platform.

Cyclic voltammetry (CV) was employed to examine the electrochemical behaviors of these pyrrole fluorophores. CV graphs were obtained with positive scan from −1 to 1.0 V using materials with 0.10 M of tetrabutylammonium perchlorate (TBAP) in anhydrous CH_2Cl_2 solution. The potentials for oxidation were determined to be 0.74–1.17 V (Fig. 3). Except BAPy, the oxidation potentials of other pyrroles exhibited insignificant variations by modifying the peripheral aryl substituents. Evidently, the oxidation potential of the pyrrole BAPy reduced slightly by introducing methoxy group onto the peripheral phenyl group. By introducing arylamino group onto the phenyl group at 3- and 4-position in the pyrrole core, these fluorophores would generate lower oxidation potentials. Based on the onset potential for the oxidation and the band gap determined from the optical absorption threshold, the HOMO and LUMO energy levels of the flourophores were estimated with regard to the energy level of the ferrocene reference (4.8 eV below the vacuum level).[17] HOMO energy, LUMO energy, and band gaps are shown in Table 1. The peripheral aryl groups of the pyrrole fluorophores also affected the photophysical and electrochemical properties. Fluorophores TPPy, BPPy, and BNPy possess similar chemical structures and HOMO levels. By replacing phenyl with naphthyl groups in the periphery of the pyrrole platform, the LUMO level was lowered because of its small energy bandgap. After amination, the HOMO levels of the fluorophores NPAPPy, NPAAPy, and NPANPy were enhanced significantly. This is because these aminated fluorophores generated lower oxidation potentials.

2.3. Molecular architecture and thermal properties

Thermal properties of the pyrrole fluorophores were analyzed by DSC and TGA (Fig. 4). By introducing phenyl groups onto the pyrrole platform, fluorophore TPPy

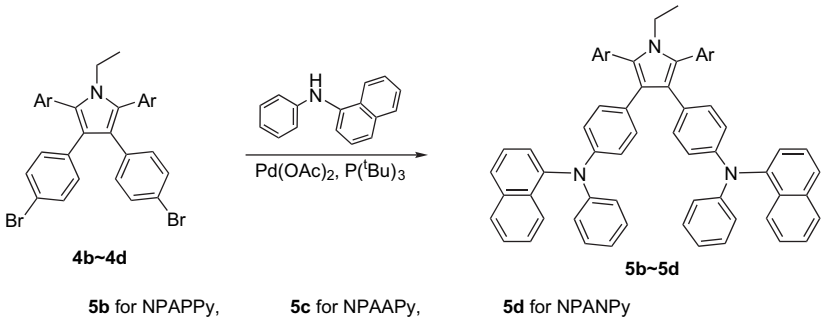

Scheme 2. Amination of aryl-substituted pyrrole fluorophores.

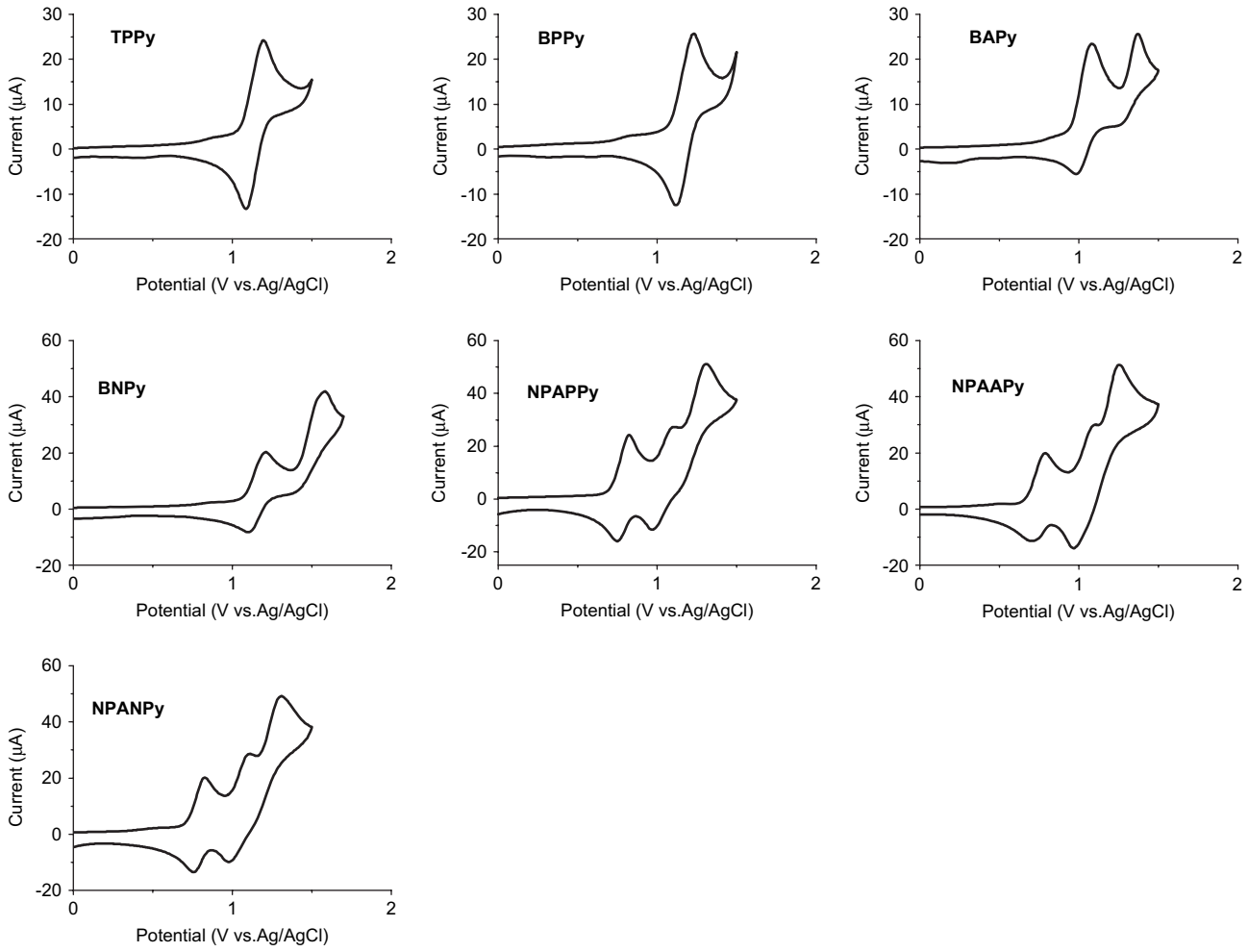

Figure 3. The reduction cyclic voltammograms of pyrrole-containing fluorophores. The result was measured in a three electrode compartment cell with a Pt wire counter electrode and an Ag/AgCl (0.1 M) reference electrode at a scan rate of 50 mV s^{-1}. The electrolyte was TBAP (tetrabutylammonium perchlorate) (0.1 M) in dichloromethane solvent.

exhibited a broad melting peak. As compared with model compound TPPy, the introduction of bromo or methoxy group onto the peripheral aryl groups would enhance the thermal stabilities of BPPy and BAPy. This implies that strong intermolecular interactions among polar anisoles or bromophenyl groups would certainly impart the BAPy and BPPy molecules with higher melting points (T_ms) and degradation temperatures (T_ds). In addition, fluorophore BNPy exhibited a conspicuous glass transition at 110 °C because the coplanarity of the pyrrole platform was disrupted by the incorporation of naphth-2-yl groups. After the introduction of naphthylphenylamino group, the glassy morphology

Table 1. Thermal and photophysical characteristics of the fluorophores

	TPPy	BPPy	BAPy	BNPy	NPAPPy	NPAAPy	NPANPy
λ_{max}^{abs}/nm[a]	256	260	258	268	306	304	309
λ_{max}^{em}/nm[a]	385	392	401	413	455	458	452
E_{gap}^{oxd}/eV[b]	3.54	3.59	3.49	3.02	2.58	2.59	2.61
ϕ_{em}[c]	0.19	0.20	4×10^{-3}	0.39	0.25	0.19	0.40
$E_{1/2}^{ox}$/eV[d]	1.14	1.17	1.03	1.16	0.79, 1.04	0.74, 1.04	0.79, 1.04
HOMO/eV[e]	5.40	5.43	5.29	5.42	5.05	5.00	5.05
LUMO/eV[e]	1.86	1.84	1.80	2.40	2.47	2.41	2.44
T_g/°C[f]	—	—	—	110	108	106	118
T_m/°C[f]	160	242	260	268	—	—	—
T_d/°C[f]	248	300	295	336	407	415	419

[a] Photophysical properties of the molecules in ethyl acetate solution were examined by UV–vis spectra and fluorescence.
[b] Estimated from the tail of the absorption spectra. $1240/\lambda_{cut\text{-}off}=E_{gap}$.
[c] Quantum yield was measured with reference to Coumarin 1 (99%) in ethyl acetate.
[d] Determined from cyclic voltammetry in dichloromethane.
[e] HOMO calculated from CV potentials using ferrocene as standard [HOMO=4.8+($E_{1/2}^{ox}-E_{1/2}^{FC}$)]. LUMO derived from the relationship LUMO=HOMO−E_{gap}.
[f] T_g, T_m were measured from DSC at a heating rate of 10 °C min^{-1}; T_ds were defined as weight loss at 5 wt %, which was measured by TGA at a heating rate of 10 °C min^{-1}.

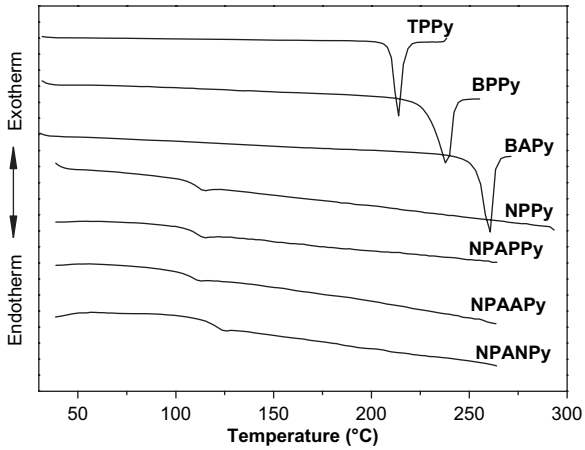

Figure 4. DSC thermograms of pyrrole-containing fluorophores from second heating cycle at 10 °C min^{-1}.

was stabilized. For fluorophores NPAPPy, NPAAPy, and NPANPy, no melting point was observed in the range from room temperature to T_ds.

The molecular framework of the aryl-substituted pyrroles can be unambiguously confirmed by single crystal X-ray diffraction analysis. Figure 5a shows the single crystal X-ray crystallographic structure of the fluorophore BPPy. The dihedral angle in the pyrrole platform (C1–C2–C3–C4) was 0.2°. This indicates that the pyrrole platform is planar. The dihedral angles between pyrrole platform and phenyl substituents at C1 (C2–C1–C7–C8) and C4 (C3–C4–C25–C26) are 124° and 116°, respectively, whereas the dihedral angles between pyrrole platform and phenyl substituents at C2 and C3 are 135° (C1–C2–C13–C18) and 123° (C2–C3–C19–C24), respectively. According to the X-ray data, all the peripheral phenyl groups were connected with the pyrrole platform in a twisted manner. This would lead to amorphism, which facilitates the fabrication of devices. Figure 5b shows the molecules of the fluorophore BPPy interlaced with each other in a bimolecular style in the lattice cell. This result indicates that the peripheral phenyl groups not only restrict the packing of the molecules, but disturb the crystal style as well. The crystal morphology accounts for the formation of glass state for the fluorophores BNPy, NPABPy, NPAAPy, and NPANPy. Because of the incorporation of various aryl substituents onto the pyrrole platforms, the number of

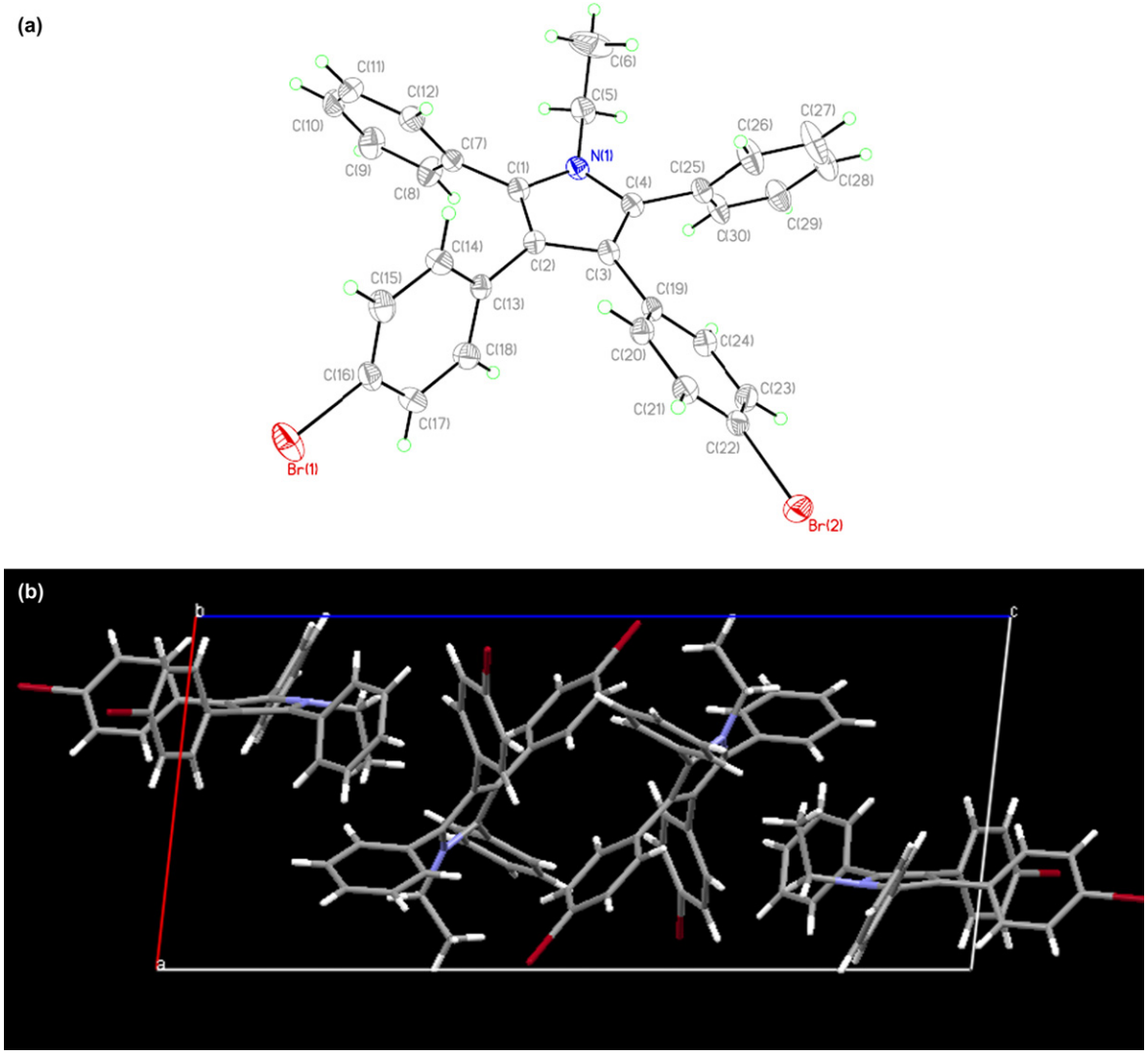

Figure 5. Single crystal X-ray diffraction pattern of fluorophore BPPy (a) and its crystal cell (b).

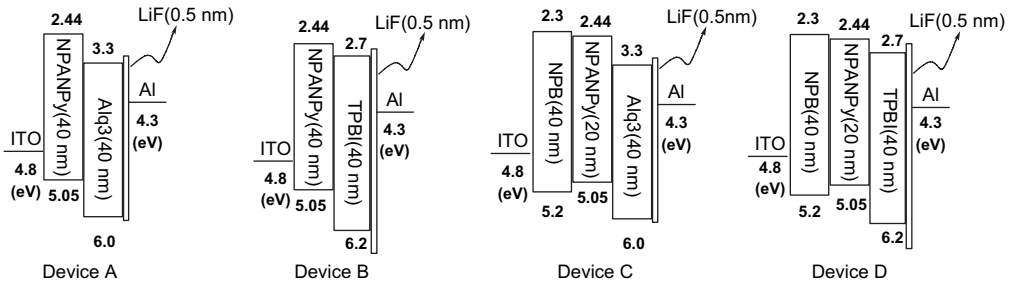

Figure 6. Energy level of the double-layer and triple-layer devices using fluorophore NPANPy as emitting layer, NPB as hole-transporting layer, Alq_3 or TPBI as electron-transporting layer, and LiF as buffer layer.

conformers for these fluorophores would increase. These polymorphic fluorophores with a nonplanar structure exhibited less tendency to pack into crystal lattice, and hence, favored amorphous morphology.[18]

2.4. Device fabrication and EL performance

According to the study of Photophysical Properties and Energy Level, fluorophore NPANPy is a promising material for OLED applications. In order to understand the capacity of the fluorophore NPANPy, double-layer and triple-layer devices were fabricated (Fig. 6). In double-layer device, fluorophore NPANPy was used as hole-transporting layer, and Alq_3 (tris(8-quinolinolato)aluminum) and TPBI (1,3,5-tris(*N*-phenylbenzimidazol-2-yl)benzene) were used as electron-transporting layers for devices A and B, respectively. In triple-layer, fluorophore NPANPy was inserted between hole-transporting layer NPB (4,4′-bis(*N*-naphth-1-yl-*N*-phenylamino)-biphenyl) and electron-transporting layers Alq_3 and TPBI for devices C and D, respectively. The configuration and energy levels of the double-layer and triple-layer devices are shown in Figure 6.

After applying voltage on these devices, devices B and D emitted blue light with maximum emission wavelength around 460 nm, and devices A and C emit green light with maximum emission wavelength around 525 nm. Figure 7 shows the electroluminescence spectra of the double-layer and triple-layer devices. The Commission International de l'Éclairage (CIE) chromaticity coordinates (x, y) for devices A, B, C, and D at an operating voltage of 8 V are (0.29, 0.57), (0.16, 0.14), (0.30, 0.56), and (0.16, 0.17), respectively. This result indicates that fluorophore NPANPy and Alq_3 acted as hole-transporting layer and electron-transporting layer, respectively. The light-emission was predominated by Alq_3. On the other hand, fluorophore NPANPy served not only as hole-transporting layer, but as emitting layer as well, when TPBI played the role as electron-transporting layer. This phenomenon could be specified by their energy levels (Fig. 6). In devices B and D, TPBI functioned as an effective hole-blocker, due to the large barrier for holes to cross from the HOMO of NPANPy to the HOMO of TPBI. Therefore, the excitons were confined in the NPANPy layer. On the contrary, a larger barrier for electrons to cross from the LUMO of Alq_3 to the LUMO of NPANPy confined the excitons in the Alq_3 layer. From these results, it is concluded that fluorophore NPANPy is capable of acting as hole-transporting material or hole-transporting/emitting material according to the electron-transporting material.

Figures 8 and 9 show the current density–voltage (I–V) and luminance–current density (L–I) characteristics of the NPANPy-based devices. Devices B and D emitted blue light with the maximum brightness of 3602 and 4748 cd m^{-2} at 10.5 and 9.5 V, respectively, when the fluorophore NPANPy served as the hole-transporting/emitting material. Devices A and C emitted green light with the maximum brightness of 43,226 and 49,505 cd m^{-2} at 10.5 and 11.5 V, respectively, when the fluorophore NPANPy served as the

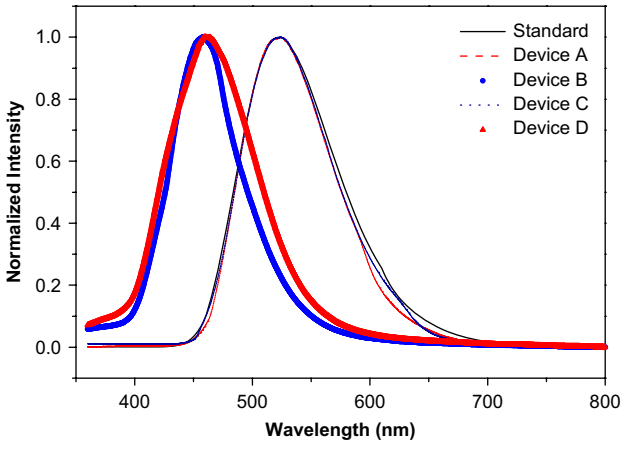

Figure 7. Electroluminescence spectra of the double-layer and triple-layer devices using fluorophore NPANPy as emitting layer.

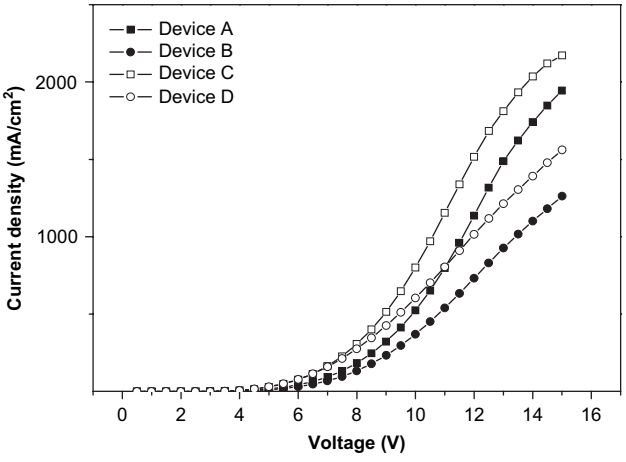

Figure 8. Current density–voltage characteristics of the NPANPy-based devices.

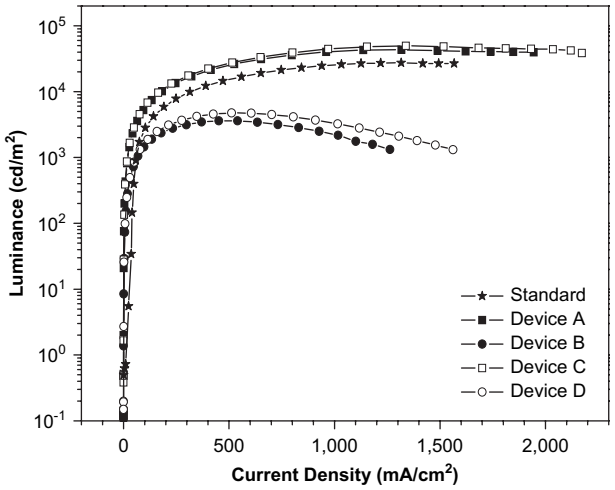

Figure 9. Luminance–current density characteristics of the NPANPy-based devices.

hole-transporting material. The device performance parameters are summarized in Table 2. It is important to note that the brightness of devices A and C is larger than standard device (maximum brightness 27,292 cd m^{-2} at 13.5 V), which was fabricated using NPB as hole-transporting layer and Alq_3 as electron-transporting/emitting layer. Especially, better device performance was found at low current density (Table 2). This implies that fluorophore NPANPy is a better hole-transporting material as compared with fluorophore NPB.

3. Conclusion

A series of novel aryl-substituted pyrroles were synthesized. Fluorescence and film-forming properties were enhanced by grafting various aryl groups onto the pyrrole platforms. These crowded peripheral aryl groups would be able to restrict the packing of these fluorophores effectively. Moreover, these molecules interlaced with each other in the lattice cell. Consequently, these fluorophores could effectively prevent the formation of aggregates, resulting in higher quantum efficiency and a stable emission spectrum in the solid film. In addition, these asymmetric peripheral aryl groups would make these fluorophores possess a number of conformers and subsequently led to stable amorphous glass morphology. In one example, fluorophore NPANPy was capable of serving as hole-transporting material or hole-transporting/emitting material. Devices B and D would emit blue light when the fluorophore NPANPy acted as hole-transporting/emitting material. Their CIE coordinate is around (0.16, 0.14), whereas the maximum brightness of 4300–5000 cd m^{-2} could be achieved. Better device performances, especially in low current density, were found in devices A and C (NPANPy as the hole-transporting material) as compared with the standard device consisting of NPB as hole-transporting material and Alq_3 as electron-transporting material.

4. Experimental

4.1. General

^1H and ^{13}C NMR spectra were recorded on Varian Gemini NMR 300 and 75.5 MHz. Thin-layer chromatography was performed using commercially prepared 60-mesh silica gel plates (Whatman K6F), and visualization was effected with short wavelength UV light (254 nm). High resolution mass spectra were recorded on a Finnigan/Thermo Quest MAT mass spectrometer. Differential scanning calorimetry (DSC) and thermogravimetric analysis (TGA) were performed using a SEIKO SII Model SSC5200 unit at heating and cooling rates of 10 °C min^{-1}. All melting points are uncorrected. UV–vis spectra were measured using a SHIMADZU UV mini-1240 spectrophotometer. Photoluminescence spectra were obtained using an Acton Research Spectra Pro-150 luminescence spectrometer. Cyclic voltammetry (CV) spectra were measured using a PGSTAT30, Eco

Table 2. Performance of the NPANPy-based OLEDs

	Standard device	Device A	Device B	Device C	Device D
Turn-on voltage (V_{on})/V[a]	2.5	2.5	3.0	2.5	3.0
Maximum brightness (L_{max})/cd m^{-2}	27,292 (at 13.5 V)	43,226 (at 12.5 V)	3602 (at 10.5 V)	49,505 (at 11.5 V)	4748 (at 9.5 V)
Maximum external quantum efficiency ($\eta_{ext,\ max}$)/%	0.95	1.69	1.45	1.82	1.37
Maximum current efficiency ($\eta_{c,\ max}$)/cd/A	3.15	5.58	1.54	5.95	1.68
Maximum power efficiency ($\eta_{p,\ max}$)/lm/W	1.44	4.77	0.92	6.46	1.14
$CIE_{x,y}$[b]	(0.31, 0.55)	(0.29, 0.57)	(0.16, 0.14)	(0.30, 0.56)	(0.16, 0.17)
λ_{max}^{EL}/nm[b]	524	525	458	524	460
FWHM/nm[b]	96	99	70	91	90
Voltage/V[c]	3.4 (5.9)	5.2 (7.1)	5.5 (7.5)	4.7 (6.3)	4.6 (6.3)
Brightness (L)/cd m^{-2}[c]	4 (2711)	1040 (5557)	297 (1483)	1122 (5943)	320 (1651)
External quantum efficiency (η_{ext})/%[c]	0.01 (0.81)	1.57 (1.69)	1.39 (1.40)	1.71 (1.82)	1.30 (1.35)
Current efficiency (η_c)/cd/A[c]	0.02 (2.7)	5.05 (5.58)	1.48 (1.48)	5.58 (5.94)	1.59 (1.65)
Power efficiency (η_p)/lm/W[c]	0.02 (1.42)	3.15 (2.47)	0.84 (0.62)	3.77 (2.96)	1.08 (0.88)

Standard device: ITO/NPB (40 nm)/Alq_3 (40 nm)/LiF/Al.
Device A: ITO/NPANPy (40 nm)/Alq_3 (40 nm)/LiF/Al.
Device B: ITO/NPANPy (40 nm)/TPBI (40 nm)/LiF/Al.
Device C: ITO/NPB (40 nm)/NPANPy (20 nm)/Alq_3 (40 nm)/LiF/Al.
Device D: ITO/NPB (40 nm)/NPANPy (20 nm)/TPBI (40 nm)/LiF/Al.
[a] Recorded at 2 cd m^{-2}.
[b] Recorded at 8 V.
[c] Recorded at 20 mA cm^{-2}, the data in parentheses were recorded at 100 mA cm^{-2}.

Chemie electrochemical analyzer operated at a scan rate of 50 mV s^{-1}; the solvent was anhydrous CH_2Cl_2 and 0.1 M tetrabutylammonium perchlorate (TBAP) was the supporting electrolyte. The potentials were measured against an Ag/Ag^+ (0.01 M $AgNO_3$) reference electrode using ferrocene as an internal standard. 1,2-Diphenylethanone (deoxybenzoin; **1a**) and other reagents were used directly as received unless otherwise noted.

4.1.1. Preparation of aryl-substituted pyrrole derivatives.

4.1.1.1. General procedure for preparation of the 1,2-diarylethanones (1). 2-Arylacetic acid (4.65 mmol) was suspended in thionyl chloride (3 mL). The suspension solution was dissolved at elevated temperatures. The solution was refluxed for 3 h. Excess of thionyl chloride was distilled and dried under vacuum. The resultant brown oil was dissolved in anhydrous dichloromethane (5 mL), and then aryl derivatives were added to the solution at 0 °C. Anhydrous $AlCl_3$ (0.8 g; 6.0 mmol) was added in small portions at the same temperature, and stirring was continued for 30 min. The reaction mixture was then refluxed for 2 h. The mixture solution was poured into a mixture of crushed ice (~5 g) and 12 M HCl (0.8 mL). The aqueous layer of the mixture was extracted with ethyl acetate (EA; 3×20 mL). The combined organic solution was washed with saturated aqueous $NaHCO_3$ (1×100 mL), dried over anhydrous $MgSO_4$, and filtered off. The solvent was then evaporated under reduced pressure. Further purification was performed by column chromatography on silica gel to afford the corresponding product.

*4.1.1.1.1. 2-(4-Bromophenyl)-1-phenylethanone (**1b**).* 2-(4-Bromophenyl)acetic acid (1.05 g; 4.89 mmol) and benzene (0.42 g; 5.4 mmol) were employed. Purification by column chromatography (EA/*n*-hexane=1/9) afforded 1.17 g (yield: 87%) of the product as a clear liquid. ^{1}H NMR ($CDCl_3$) δ 4.42 (s, 2H), 7.14 (dd, J=2.4, 8.4 Hz, 2H), 7.44–7.49 (m, 4H), 7.55 (t, J=7.2 Hz, 1H), 7.99 (dd, J=2.4, 6.6 Hz, 2H). ^{13}C NMR ($CDCl_3$) δ 44.50, 55.50, 113.88, 120.84, 129.41, 130.86, 131.18, 131.70, 133.88, 163.68, 195.58. HRMS (FAB) *m/z* calcd for $C_{14}H_{11}BrO$: 273.9993. Found: 273.9992.

*4.1.1.1.2. 2-(4-Bromophenyl)-1-(4-methoxyphenyl)ethanone (**1c**).* 2-(4-Bromophenyl)acetic acid (0.83 g; 3.86 mmol) and anisole (0.46 g; 4.25 mmol) were employed. Purification by column chromatography (EA/*n*-hexane=1/9) afforded 1.02 g of the product as a clear liquid (yield: 87%). ^{1}H NMR ($CDCl_3$) δ 3.87 (s, 3H), 4.19 (s, 2H), 6.93 (d, J=8.7 Hz), 7.14 (d, J=8.1 Hz, 2H), 7.44 (d, J=8.4 Hz, 2H), 7.97 (d, J=9.0 Hz, 2H). ^{13}C NMR ($CDCl_3$) δ 44.49, 55.49, 113.87, 120.83, 129.41, 130.86, 131.17, 131.70, 133.87, 163.68, 195.58. HRMS (FAB) *m/z* calcd for $C_{15}H_{13}BrO_2$: 304.0099. Found: 304.0097.

*4.1.1.1.3. 2-(4-Bromophenyl)-1-(naphthalen-2-yl)ethanone (**1d**).* 2-(4-Bromophenyl)acetic acid (0.98 g; 4.56 mmol) and naphthalene (0.64 g; 5.0 mmol) were employed. Purification by column chromatography (EA/*n*-hexane=1/9) afforded 1.21 g of the product as a clear liquid (yield: 82%). ^{1}H NMR ($CDCl_3$) δ 4.19 (s, 2H), 7.19 (d, J=8.1 Hz, 2H), 7.46 (d, J=8.4 Hz, 2H), 7.59 (m, 2H), 7.88 (t, 2H), 7.97 (d, J=7.8 Hz, 1H), 8.04 (d, J=6.9 Hz, 1H), 8.52 (s, 1H). ^{13}C NMR ($CDCl_3$) δ 44.78, 120.97, 124.07, 126.88, 127.78, 128.62, 128.67, 129.58, 130.29, 131.26, 131.75, 132.46, 133.56, 133.73, 135.65, 196.94. HRMS (FAB) *m/z* calcd for $C_{18}H_{13}BrO$: 324.0150. Found: 324.0153.

4.1.1.2. General procedure for preparation of the 1,2,3,4-tetraarylbutane-1,4-diones (2). Potassium *tert*-butoxide 0.41 g (3.65 mmol) was dissolved in 10 mL anhydrous THF. The solution was cooled down to −60 °C. 1,2-Diarylethanone derivatives in 10 mL anhydrous THF were then added dropwise to the solution. Subsequently, iodine (0.93 g, 3.63 mmol) in anhydrous THF (20 mL) was added. The reaction temperature was recovered to 0 °C, and the mixture was stirred for 2 h. Aqueous sodium bisulfite (1 M) was added to terminate the reaction. The aqueous layer of the mixture was extracted with EA (3×20 mL). The combined organic solution was washed with brine (2×20 mL), deionized water, dried over anhydrous $MgSO_4$, and filtered off. The solvent was then evaporated under reduced pressure. Further purification was performed by column chromatography on silica gel to afford the corresponding product.

*4.1.1.2.1. 1,2,3,4-Tetraphenylbutane-1,4-dione (**2a**).* Deoxybenzoin (**1a**; 1.00 g) was employed. Purification by column chromatography (EA/*n*-hexane=1/5) afforded 0.73 g of the product in the form of white powder (73%). ^{1}H NMR ($CDCl_3$) δ 5.78 (s, 2H), 7.10 (t, J=7.5 Hz, 2H), 7.21 (t, J=7.5 Hz, 4H), 7.32 (t, J=7.5 Hz, 4H), 7.44 (t, J=7.5 Hz, 2H), 7.53 (d, J=6.9 Hz, 4H), 7.86 (d, J=6.9 Hz, 4H). ^{13}C NMR ($CDCl_3$) 56.19, 127.36, 128.44, 128.45, 128.77, 129.06, 132.93, 136.88, 198.39. HRMS (FAB) *m/z* calcd for $C_{28}H_{22}O_2$: 390.1260. Found: 391.1708 (M^++H).

*4.1.1.2.2. 2,3-Bis(4-bromophenyl)-1,4-diphenylbutane-1,4-dione (**2b**).* 2-(4-Bromophenyl)-1-phenylethanone (**1b**; 0.98) was employed. Purification by column chromatography (EA/*n*-hexane=1/5) afforded the product as white powder (0.79 g; yield: 81%). ^{1}H NMR ($CDCl_3$) δ 5.32 (s, 2H), 6.90 (d, J=8.4 Hz, 4H), 7.27 (t, J=8.7 Hz, 4H), 7.38 (t, J=7.2 Hz, 4H), 7.49 (t, J=7.2 Hz, 2H), 7.94 (d, J=7.2 Hz, 4H). ^{13}C NMR ($CDCl_3$) δ 57.57, 121.63, 128.58, 128.84, 130.36, 132.04, 133.24, 135.12, 135.98, 198.80. HRMS (FAB) *m/z* calcd for $C_{28}H_{20}Br_2O_2$: 545.9830. Found: 546.9907 [M^++H].

*4.1.1.2.3. 2,3-Bis(4-bromophenyl)-1,4-bis(4-methoxyphenyl)butane-1,4-dione (**2c**).* 2-(4-Bromophenyl)-1-(4-methoxyphenyl)ethanone (**1c**; 0.92 g) was employed. Purification by column chromatography (EA/*n*-hexane=1/5) afforded the product as white powder (0.77 g; yield: 84%). ^{1}H NMR ($CDCl_3$) δ 3.81 (s, 3H), 5.28 (s, 1H), 6.84 (d, J=7.8 Hz, 2H), 6.89 (d, J=7.8 Hz, 2H), 7.27 (d, J=7.5 Hz, 2H), 7.92 (d, J=7.8 Hz, 2H). ^{13}C NMR ($CDCl_3$) δ 55.42, 57.11, 113.75, 121.39, 128.96, 130.30, 131.19, 131.91, 135.72, 163.52, 197.15. HRMS (FAB) *m/z* calcd for $C_{30}H_{24}Br_2O_4$: 606.0041. Found: 607.0125 (M^++H). Anal. Calcd for $C_{36}H_{24}Br_2O_2$: C, 59.23; H, 3.98. Found: C, 58.65; H, 3.89.

*4.1.1.2.4. 2,3-Bis(4-bromophenyl)-1-(naphthalen-2-yl)-4-(naphthalen-3-yl)butane-1,4-dione (**2d**).* 2-(4-Bromophenyl)-1-(naphthalen-2-yl)ethanone (**1d**; 1.10 g) was

employed. Purification by column chromatography (EA/*n*-hexane=1/5) afforded the product as white powder (0.94 g; yield: 86%). ^{1}H NMR ($CDCl_3$) δ 5.55 (s, 2H), 7.02 (d, *J*=8.1 Hz, 4H), 7.31 (d, *J*=8.1 Hz, 4H), 7.48–7.59 (m, 4H), 7.82 (d, *J*=9.0 Hz, 4H), 7.91 (d, *J*=7.8 Hz, 2H), 7.99 (d, *J*=8.7 Hz, 2H). ^{13}C NMR ($CDCl_3$) δ 57.71, 121.67, 124.38, 126.71, 127.68, 128.45, 128.59, 129.70, 130.42, 130.77, 132.09, 132.42, 133.35, 135.29, 135.60, 198.80. HRMS (FAB) *m/z* calcd for $C_{36}H_{24}Br_2O_2$: 646.0143. Found: 647.0217 (M^++H).

4.1.1.3. General procedure for preparation of the 2,3,4,5-tetraarylpyrroles (3). Ammonium acetate (6.49 mmol) and tetraarylbutane-1,4-dione (1.83 mmol, 1.0 equiv) were dissolved in 10 mL acetic acid. The mixture was heated to 130 °C and kept stirring at this temperature for 24 h. When the reaction was completed, the solution was poured into 100 mL deionized water. After filtering the precipitate, the crude solid was dissolved in EA (20 mL). The EA solution was washed with saturated sodium carbonate (2×20 mL) and deionized water (2×20 mL), dried over anhydrous $MgSO_4$, and filtered off. The solvent was then evaporated under reduced pressure. Further purification was performed by column chromatography on silica gel to afford the corresponding product.

*4.1.1.3.1. 2,3,4,5-Tetraphenylpyrrole (**3a**).* 1,2,3,4-Tetraphenylbutane-1,4-dione (**2a**; 0.72 g) was employed. Purification by column chromatography (EA/*n*-hexane=1/13) afforded the product as white powder (0.52 g; yield: 76%). ^{1}H NMR ($CDCl_3$) δ 7.10–7.27 (m, 20H), 8.40 (s, 1H). ^{13}C NMR ($CDCl_3$) δ 123.20, 125.84, 125.92, 126.64, 127.13, 127.87, 128.82, 128.82, 128.58, 130.38, 130.96, 132.71, 135.35. HRMS (FAB) *m/z* calcd for $C_{28}H_{21}N$: 371.1674. Found: 371.1681.

*4.1.1.3.2. 3,4-Bis(4-bromophenyl)-2,5-diphenyl-1H-pyrrole (**3b**).* 2,3-Bis(4-bromophenyl)-1,4-diphenylbutane-1,4-dione (**2b**; 0.99 g) was employed. Purification by column chromatography (EA/*n*-hexane=1/13) afforded 0.71 g (74%) of the product as white powder. ^{1}H NMR ($CDCl_3$) δ 6.84 (d, *J*=8.1 Hz, 4H), 7.18–7.24 (m, 14H), 8.37 (s, 1H). ^{13}C NMR ($CDCl_3$) δ 120.24, 127.30, 128.78, 131.26, 132.51, 134.10. HRMS (FAB) *m/z* calcd for $C_{28}H_{19}Br_2N$: 526.9884. Found: 526.9886.

*4.1.1.3.3. 3,4-Bis(4-bromophenyl)-2,5-bis(4-methoxyphenyl)-1H-pyrrole (**3c**).* 2,3-Bis(4-bromophenyl)-1,4-bis(4-methoxyphenyl)butane-1,4-dione (**2c**; 0.82 g) was employed. Purification by column chromatography (EA/*n*-hexane=1/13) afforded the product as white powder (0.49 g; yield: 62%). ^{1}H NMR ($CDCl_3$) δ 3.81 (s, 3H), 6.83 (d, *J*=8.7 Hz, 2H), 6.99 (d, *J*=8.4 Hz, 2H), 7.39 (dd, *J*=2.4, 8.7 Hz, 4H). ^{13}C NMR ($CDCl_3$) δ 55.24, 113.92, 119.25, 124.92, 128.87, 129.19, 131.10, 132.92, 135.41, 158.15. HRMS (FAB) *m/z* calcd for $C_{30}H_{23}Br_2NO_2$: 587.0096. Found: 587.0100. Anal. Calcd for $C_{30}H_{23}Br_2NO_2$: C, 61.14; H, 3.93; N, 2.38. Found: C, 61.27; H, 4.08; N, 2.03.

*4.1.1.3.4. 3,4-Bis(4-bromophenyl)-2,5-bis(naphthalen-2-yl)-1H-pyrrole (**3d**).* 2,3-Bis(4-bromophenyl)-1-(naphthalen-2-yl)-4-(naphthalen-3-yl)butane-1,4-dione (**2d**; 0.91 g) was employed. Purification by column chromatography (EA/*n*-hexane=1/13) afforded the product as white powder (0.66 g; yield: 75%). ^{1}H NMR ($CDCl_3$) δ 6.98 (d, *J*=8.1 Hz, 6H), 7.32 (d, *J*=8.4 Hz, 6H), 7.42–7.55 (m, 4H), 7.73–7.80 (m, 6H), 8.76 (s, 1H). ^{13}C NMR ($CDCl_3$) δ 120.39, 122.03, 126.42, 127.73, 131.32, 132.57. HRMS (FAB) *m/z* calcd for $C_{36}H_{23}Br_2N$: 627.0197. Found: 627.0199.

4.1.1.4. General procedure for preparation of the *N*-ethyl-2,3,4,5-tetraarylpyrroles (4). Sodium hydride (0.14 g, 60 wt % in mineral oil; 5.83 mol) was treated with *n*-hexane, and then suspended in dry DMAc (5 mL). The solution of tetraarylpyrrole (1.89 mmol) in dry DMAc (5 mL) was added dropwise under nitrogen atmosphere at 0 °C for 1 h. After addition of bromoethane (0.25 g; 2.29 mmol), the solution was stirred for 4 h at room temperature. Excessive sodium hydride was terminated by addition of deionized water, and the solution was subsequently extracted with EA several times. The combined organic solution was washed with deionized water several times, dried over anhydrous $MgSO_4$, and filtered off. The solvent was then evaporated under reduced pressure. Further purification was performed by column chromatography on silica gel to afford the corresponding product.

*4.1.1.4.1. 1-Ethyl-2,3,4,5-tetraphenylpyrrole (**4a**).* 2,3,4,5-Tetraphenylpyrrole (**3a**; 0.98 g) was employed. Purification by column chromatography (EA/*n*-hexane=1/19) afforded 0.91 g (86%) of the product as white powder. ^{1}H NMR ($CDCl_3$) δ 0.95–1.00 (t, *J*=7.2 Hz, 3H), 3.90 (q, *J*=7.2 Hz, 2H), 6.91–6.95 (m, 4H), 7.00–7.05 (m, 6H), 7.30–7.35 (m, 10H). ^{13}C NMR ($CDCl_3$) δ 16.61, 39.39, 122.11, 124.93, 127.33, 128.13, 130.82, 130.96, 131.43, 133.21, 135.60. HRMS (FAB) *m/z* calcd for $C_{30}H_{25}N$: 399.1987. Found: 399.1979.

*4.1.1.4.2. 3,4-Bis(4-bromophenyl)-1-ethyl-2,5-diphenyl-1H-pyrrole (**4b**).* 3,4-Bis(4-bromophenyl)-2,5-diphenyl-1*H*-pyrrole (**3b**; 1.00 g) was employed. Purification by column chromatography (EA/*n*-hexane=1/19) afforded the product as white powder (0.89 g; yield: 84%). ^{1}H NMR ($CDCl_3$) δ 0.96 (t, *J*=7.2 Hz, 3H), 3.85 (d, *J*=7.2 Hz, 2H), 6.75 (d, *J*=4.5 Hz, 4H), 7.15 (d, *J*=4.5 Hz, 4H), 7.25–7.38 (m, 10H). ^{13}C NMR ($CDCl_3$) δ 16.60, 39.45, 119.20, 120.65, 127.71, 128.34, 130.71, 131.22, 131.33, 132.26, 132.64, 134.34. HRMS (FAB) *m/z* calcd for $C_{30}H_{23}Br_2N$: 555.0197. Found: 555.0196.

*4.1.1.4.3. 3,4-Bis(4-bromophenyl)-1-ethyl-2,5-bis(4-methoxyphenyl)-1H-pyrrole (**4c**).* 3,4-Bis(4-bromophenyl)-2,5-bis(4-methoxyphenyl)-1*H*-pyrrole (**3c**; 1.12 g) was employed. Purification by column chromatography (EA/*n*-hexane=1/19) afforded the product as white powder (0.97 g; yield: 83%). ^{1}H NMR ($CDCl_3$) δ 0.97 (t, *J*=7.2 Hz, 3H), 3.83 (m, 8H), 6.76 (d, *J*=8.7 Hz, 4H), 6.88 (d, *J*=8.7 Hz, 4H), 7.16 (d, *J*=8.7 Hz, 4H), 7.21 (d, *J*=8.7 Hz, 4H). ^{13}C NMR ($CDCl_3$) δ 16.66, 39.29, 55.19, 113.78, 119.03, 120.34, 124.86, 130.68, 130.75, 132.24, 132.51, 134.58, 159.07. HRMS (FAB) *m/z* calcd for $C_{32}H_{27}Br_2NO_2$: 615.0409. Found: 615.0410. Anal. Calcd for $C_{32}H_{27}Br_2NO_2$: C, 62.25; H, 4.41; N, 2.27. Found: C, 62.23; H, 4.41; N, 1.92.

*4.1.1.4.4. 3,4-Bis(4-bromophenyl)-1-ethyl-2,5-bis(naphthalen-2-yl)-1H-pyrrole (**4d**).* 3,4-Bis(4-bromophenyl)-2,5-

bis(naphthalen-2-yl)-1*H*-pyrrole (**3d**; 1.19 g) was employed. Purification by column chromatography (EA/*n*-hexane=1/19) afforded the product as white powder (1.07 g; yield: 86%). ^{1}H NMR ($CDCl_3$) δ 0.97 (t, 3H), 3.95 (d, J=7.2 Hz, 2H), 6.82 (d, J=8.4 Hz, 4H), 7.13 (d, J=8.7 Hz, 4H), 7.39 (d, J=6.9 Hz, 2H), 7.50–7.53 (m, 4H), 7.80–7.88 (m, 8H). ^{13}C NMR ($CDCl_3$) δ 16.74, 39.65, 119.32, 121.20, 126.29, 126.38, 127.74, 127.97, 128.08, 129.07, 130.14, 130.35, 130.78, 131.31, 132.28, 132.62, 133.14, 134.26. HRMS (FAB) *m*/*z* calcd for $C_{38}H_{27}Br_2N$: 655.0510. Found: 655.0516.

4.1.2. Preparation of the 3,4-bis(4-1-naphthylanilinophenyl)-1-ethyl-2,5-diaryl-1*H*-pyrrole. A single necked 100-mL round-bottomed flask was charged with the naphth-1-ylphenylamine (0.438 g, 2 mmol), dibromoetraarylpyrrole (**4b**–**4d**) (1 mmol), palladium(II) acetate (0.033 g, 0.05 mmol), and tri-*tert*-butylphosphine (0.02 g, 0.1 mmol). Dry toluene (5 mL) and sodium *tert*-butoxide (0.023 g, 0.24 mmol) were added and heated at 110 °C for 24 h under a nitrogen atmosphere. After cooling, the mixture was quenched with water and the solution was then extracted with dichloromethane (3×50 mL). The combined organic solution was washed with water, dried over anhydrous $MgSO_4$, and filtered off. Evaporation of volatiles left a dark solid. Further purification was performed by column chromatography on silica gel to afford the corresponding product.

4.1.2.1. 1-Ethyl-3,4-bis(4-1-naphthylanilinophenyl)-2,5-di(naphthalen-2-yl)-1*H*-pyrrole (5b). 3,4-Bis(4-bromophenyl)-1-ethyl-2,5-diphenyl-1*H*-pyrrole (**4b**; 0.56 g) was employed. Purification by column chromatography (EA/*n*-hexane=1/19) afforded the product as white powder (0.64 g; yield: 76%). ^{1}H NMR (500 MHz, DMSO-d_6): δ 0.773 (t, J=7.0 Hz, 3H), 3.753 (q, J=7.0 Hz, 2H), 6.598 (d, J=8.5 Hz, 4H), 6.721 (d, J=7.0 Hz, 4H), 6.770 (d, J=8.0 Hz, 4H), 6.877 (t, J=7.5 Hz, 2H), 7.118 (t, J=7.5 Hz, 4H), 7.200 (t, J=7.5 Hz, 2H), 7.227 (d, J=7.0 Hz, 4H), 7.325 (m, 10H), 7.385 (t, J=7.5 Hz, 2H), 7.469 (t, J=8.0 Hz, 2H), 7.687 (d, J=8.5 Hz, 2H), 7.829 (d, J=8.5 Hz, 2H), 7.926 (d, J=8.0 Hz, 2H). ^{13}C NMR (500 MHz, DMSO-d_6): δ 16.051, 120.538, 120.705, 121.310, 121.711, 123.461, 126.143, 126.260, 126.544, 127.018, 127.456, 128.199, 128.498, 129.176, 129.329, 130.240, 130.532, 131.028, 131.312, 132.595, 134.906, 142.692, 144.922, 147.838. HRMS (FAB) *m*/*z* calcd for $C_{62}H_{47}N_3$: 834.0567. Found: 833.3766 [M^+].

4.1.2.2. 1-Ethyl-3,4-bis(4-1-naphthylanilinophenyl)-2,5-di(naphthalen-2-yl)-1*H*-pyrrole (5c). 3,4-Bis(4-bromophenyl)-1-ethyl-2,5-bis(4-methoxyphenyl)-1*H*-pyrrole (**4c**; 0.62 g) was employed. Purification by column chromatography (EA/*n*-hexane=1/19) afforded the product as white powder (0.66 g; yield: 74%). ^{1}H NMR (500 MHz, DMSO-d_6): δ 0.93 (t, J=11 Hz, 3H), 3.82 (m, 8H), 6.73 (q, J=9.0 Hz, 8H), 6.86 (dd, J=9.0, 12.5 Hz, 6H), 6.93 (d, J=8.0 Hz, 4H), 7.12 (t, J=8.0 Hz, 4H), 7.18 (t, J=8.5 Hz, 2H), 7.24 (d, J=8.5 Hz, 6H), 7.33 (t, J=7.5 Hz, 2H), 7.39 (t, J=7.5 Hz, 2H), 7.70 (d, J=7.5 Hz, 2H), 7.81 (d, J=8.5 Hz, 4H). ^{13}C NMR (500 MHz, DMSO-d_6): δ 16.62, 39.21, 55.14, 113.47, 121.25, 121.69, 124.50, 125.68, 125.93, 126.23, 126.91, 128.20, 128.86, 129.81, 129.99, 131.14, 131.39, 132.51, 135.20, 143.81, 145.25, 148.63, 158.66. HRMS (FAB) *m*/*z* calcd for $C_{64}H_{51}N_3O_2$: 893.3981. Found: 893.3978 [M^+].

4.1.2.3. 1-Ethyl-3,4-bis(4-1-naphthylanilinophenyl)-2,5-di(naphthalen-2-yl)-1*H*-pyrrole (5d). 1-Ethyl-3,4-bis(4-bromophenyl)-2,5-bis(naphthalen-2-yl)-1*H*-pyrrole (**4d**; 0.66 g) was employed. Purification by column chromatography (EA/*n*-hexane=1/19) afforded the product as white powder (0.68 g; yield: 73%). ^{1}H NMR (500 MHz, DMSO-d_6): δ 0.788 (t, J=7.0 Hz, 3H), 3.924 (q, J=7.0 Hz, 2H), 6.593 (d, J=8.5 Hz, 4H), 6.738 (d, J=7.5 Hz, 4H), 6.811 (d, J=8.5 Hz, 4H), 6.855 (t, J=7.5 Hz, 2H), 7.099 (t, J=7.5 Hz, 4H), 7.190 (m, 4H), 7.374 (t, J=7.0 Hz, 2H), 7.438 (m, 4H), 7.532 (m, 4H), 7.663 (d, J=9.0 Hz, 2H), 7.802 (d, J=8.5 Hz, 2H), 7.84–7.92 (m, 10H). ^{13}C NMR (500 MHz, DMSO-d_6): δ 16.117, 120.676, 120.749, 121.318, 122.433, 123.432, 126.100, 126.238, 126.289, 126.493, 126.916, 127.543, 127.893, 128.462, 129.140, 129.293, 130.022, 130.452, 130.576, 131.429, 131.961, 132.763, 134.870, 142.677, 145.068, 147.838. HRMS (FAB) *m*/*z* calcd for $C_{70}H_{51}N_3$: 933.4083. Found: 933.4090.

4.2. Fabrication of Organic Light-Emitting Devices (OLEDs) and measurement

The OLED device was fabricated by use of vacuum deposition of NPB, NPANPy, TPBI or Alq_3, LiF, and the Al electrode on top of the ITO glass substrate. The device structure was made by ITO/NPB (20 nm)/Cz-NPh (20 nm)/TPBI (40 nm) or Alq_3 (40 nm)/LiF (0.5 nm)/Al (150 nm), where ITO, NPB, Alq_3, TPBI were indium tin oxide, 4,4′-bis[*N*-(1-naphthyl)-*N*-phenylamino] biphenyl, tris(8-hydroxyquinolinato)aluminum(III), and 1,3,5-tris(*N*-phenyl benzimidizol-2-yl)benzene, respectively. The thermal evaporation of organic materials was carried out by use of ULVAC Cryogenics at a chamber pressure of 10^{-6} torr. Current–voltage–luminescence (*I*–*V*–*L*) characteristics and CIE color coordinates were measured simultaneously by use of a Keithley 2400 Source meter and a Newport 1835C optical meter equipped with a Newport 818-ST silicon photodiode, respectively.

Acknowledgements

Financial support by National Science Council of Taiwan is gratefully acknowledged. R.-J.J. also thanks Education Ministry of Taiwan for funding Center for Advanced Industry Technology and Precision Processing, NCHU.

Supplementary data

Supplementary data associated with this article can be found in the online version, at doi:10.1016/j.tet.2007.05.032.

References and notes

1. Tang, C. W.; Van Slyke, S. A. *Appl. Phys. Lett.* **1987**, *51*, 913.
2. Burroughes, J. H.; Bradley, D. D. C.; Brown, A. R.; Marks, R. N.; MacKay, K.; Friend, R. H.; Burn, P. L.; Holmes, A. B. *Nature* **1990**, *347*, 539.

3. (a) Chen, C. H.; Shi, J. *Coord. Chem. Rev.* **1998**, *171*, 161; (b) Hu, N. X.; Esteghamatian, M.; Xie, S.; Popovic, Z.; Hor, A. M.; Ong, B.; Wang, S. *Adv. Mater.* **1999**, *11*, 17; (c) Wang, J. F.; Jabbour, G. E.; Mash, E. A.; Anderson, J.; Zhang, Y.; Lee, P. A.; Armstrong, N. R.; Peryhambarian, N.; Kippelen, B. *Adv. Mater.* **1999**, *11*, 1266.
4. (a) Hanack, M.; Behnisch, B.; Häckl, H.; Martinez-Ruiz, P.; Schweikart, K. H. *Thin Solid Films* **2002**, *417*, 26; (b) Li, C. L.; Shien, S. J.; Lin, S. C.; Liu, R. S. *Org. Lett.* **2003**, *5*, 1131; (c) Kan, Y.; Wang, L.; Duan, L.; Hu, Y.; Wu, G.; Qiu, Y. *Appl. Phys. Lett.* **2004**, *84*, 1513; (d) Kido, J.; Kimura, M.; Nagai, K. *Science* **1995**, *267*, 1332.
5. Huang, C.; Zhen, C. G.; Su, S. P.; Loh, K. P.; Chen, Z. K. *Org. Lett.* **2005**, *7*, 391.
6. (a) Setayesh, S.; Grimsdale, A. C.; Weil, T.; Enkelmann, V.; Mullen, K.; Meghdadi, F.; List, E. J. W.; Leising, G. *J. Am. Chem. Soc.* **2001**, *123*, 946; (b) Gronheid, R.; Hofkens, J.; Kohn, F.; Weil, T.; Reuther, E.; Müllen, K.; De Schryver, F. C. *J. Am. Chem. Soc.* **2002**, *124*, 2418; (c) Freeman, A. W.; Koene, S. C.; Malenfant, P. R. L.; Thompson, M. E.; Frechet, J. M. J. *J. Am. Chem. Soc.* **2004**, *122*, 12385; (d) Justin Thomas, K. R.; Thompson, A. L.; Sivakumar, A. V.; Bardeen, C. J.; Thayumanavan, S. *J. Am. Chem. Soc.* **2005**, *127*, 373; (e) Kwon, T. W.; Alam, M. M.; Jenekhe, S. A. *Chem. Mater.* **2004**, *16*, 4657; (f) Chen, C. H.; Lin, J. T.; Yeh, M. C. P. *Org. Lett.* **2006**, *8*, 2233; (g) Lupton, J. M.; Samuel, I. D. W.; Beavington, R.; Burn, P. L.; Bassler, H. *Adv. Mater.* **2001**, *13*, 258; (h) Lo, S. C.; Male, N. A. H.; Markham, J. P. J.; Magennis, S. W.; Burn, P. L.; Salata, O. V.; Samuel, I. D. W. *Adv. Mater.* **2002**, *14*, 975; (i) Anthopoulos, T. D.; Frampton, M. J.; Namdas, E. B.; Burn, P. L.; Samuel, I. D. W. *Adv. Mater.* **2004**, *16*, 557.
7. (a) Noda, T.; Shirota, Y. *J. Am. Chem. Soc.* **1998**, *120*, 9714; (b) Noda, T.; Ogawa, H.; Shirota, Y. *Adv. Mater.* **1999**, *11*, 283; (c) Shirota, Y.; Kinoshita, M.; Noda, T.; Okumoto, K.; Ohara, T. *J. Am. Chem. Soc.* **2000**, *122*, 1102; (d) Noda, T.; Shirota, Y. *J. Lumin.* **2000**, *87*, 1168; (e) Kinoshita, M.; Kita, H.; Shirota, Y. *Adv. Funct. Mater.* **2002**, *12*, 780; (f) Doi, H.; Kinoshita, M.; Okumoto, K.; Shirota, Y. *Chem. Mater.* **2003**, *15*, 1080; (g) Uchida, M.; Ono, Y.; Yokoi, H.; Nakano, T.; Furukawa, K. *J. Photopolym. Sci. Technol.* **2001**, *4*, 306; (h) Shen, J. Y.; Lee, C. Y.; Huang, T. H.; Lin, J. T.; Tao, Y. T.; Chien, C. H.; Tsai, C. *J. Mater. Chem.* **2005**, *15*, 2455.
8. (a) Liu, X. M.; He, C.; Xu, J. W. *Tetrahedron Lett.* **2004**, *45*, 1593; (b) Liu, X. M.; He, C.; Huang, J. C. *Tetrahedron Lett.* **2004**, *45*, 6173; (c) Wang, S.; Oldham, W. J.; Hudack, R. A.; Bazan, G. C. *J. Am. Chem. Soc.* **2000**, *122*, 5695.
9. (a) Armaroli, N.; Balzani, V.; Collin, J. P.; Gavina, P.; Sauvage, J. P.; Ventura, B. *J. Am. Chem. Soc.* **1999**, *121*, 4397; (b) Fournier, J. H.; Maris, T.; Wuest, J. D.; Guo, W. Z.; Galoppini, E. *J. Am. Chem. Soc.* **2003**, *125*, 1002; (c) Chan, L. H.; Lee, R. H.; Hsieh, C. F.; Yeh, H. C.; Chen, C. T. *J. Am. Chem. Soc.* **2002**, *124*, 6469; (d) Yeh, H. C.; Lee, R. H.; Chan, L. H.; Lin, T. Y. J.; Chen, C. T.; Balasubramaniam, E.; Tao, Y. T. *Chem. Mater.* **2001**, *13*, 2788; (e) Rathore, R.; Burns, C. L.; Deselnicu, M. I. *Org. Lett.* **2001**, *3*, 2887; (f) Li, Q.; Rukavishnikov, A. V.; Petukhov, P. A.; Zaikova, T. O.; Keana, J. F. W. *Org. Lett.* **2002**, *4*, 3631; (g) Langhals, H.; Wagner, C.; Ismael, R. *New J. Chem.* **2001**, *25*, 1047; (h) Liu, X. M.; He, C.; Hao, X. T.; Tan, L. W.; Li, Y.; Ong, K. S. *Macromolecules* **2004**, *37*, 5965; (i) Liu, X. M.; He, C.; Huang, J.; Xu, J. *Chem. Mater.* **2005**, *17*, 434.
10. (a) Gensch, T.; Hofkens, J.; Heirmann, A.; Tsuda, K.; Verheijen, W.; Vosch, T.; Crist, T.; Basche, T.; Mullen, K.; De Schryver, F. C. *Angew. Chem., Int. Ed.* **1999**, *38*, 3752; (b) Pogantsch, A.; Wenl, E. G.; List, E. J. W.; Leising, G.; Mullen, K. *Adv. Mater.* **2002**, *14*, 1061; (c) Shen, W. J.; Dodda, R.; Wu, C. C.; Wu, F. I.; Liu, T. H.; Chen, H. H.; Chen, C. H.; Shu, C. F. *Chem. Mater.* **2004**, *16*, 930; (d) Wu, R. L.; Schumm, J. S.; Pearson, D. L.; Tour, J. M. *J. Org. Chem.* **1996**, *61*, 6906; (e) Tour, J. M.; Wu, R.; Schumm, J. S. *J. Am. Chem. Soc.* **1990**, *112*, 5662; (f) Wong, K. T.; Chien, Y. Y.; Chen, R. T.; Wang, C. F.; Lin, Y. T.; Chiang, H. H.; Hsieh, P. Y.; Wu, C. C.; Chou, C. H.; Su, Y. O.; Lee, G. H.; Peng, S. M. *J. Am. Chem. Soc.* **2002**, *124*, 11576; (g) Xia, C. J.; Advincula, R. C. *Macromolecules* **2001**, *34*, 5854; (h) Steuber, F.; Staudigel, J.; Stossel, M.; Simmerer, J.; Winnacker, A.; Spreitzer, H.; Weissortel, F.; Salbeck, J. *Adv. Mater.* **2000**, *12*, 130.
11. Oldham, W. J., Jr.; Lachicotte, R. J.; Bazan, G. C. *J. Am. Chem. Soc.* **1998**, *120*, 2987.
12. (a) Shi, J.; Tang, C. W.; Chen, C. H. U.S. Patent 5,645,948, 1997; (b) Sonsale, A. Y.; Gopinathan, S.; Gopinathan, C. *Indian J. Chem.* **1976**, *14*, 408.
13. Higuchi, A.; Inada, H.; Kobata, T.; Shirota, Y. *Adv. Mater.* **1991**, *3*, 549.
14. Herbich, J.; Kijak, M.; Zielinska, A.; Thummel, R. P.; Waluk, J. *J. Phys. Chem. A* **2002**, *106*, 2158.
15. Krasovitskii, B. M.; Bolotin, B. M. *Organic Luminescent Materials;* Vopian, V. G., Translator; VCH: Weinheim, Germany, 1988.
16. (a) Wolfe, J. P.; Wagaw, S.; Marcoux, J. F.; Buchwald, S. L. *Acc. Chem. Res.* **1998**, *31*, 805; (b) Hartwig, J. F. *Angew. Chem., Int. Ed.* **1998**, *37*, 2046; (c) Yamamoto, T.; Nishiyama, M.; Koie, Y. *Tetrahedron Lett.* **1998**, *39*, 2367; (d) Goodson, F. E.; Hauck, S. I.; Hartwig, J. F. *J. Am. Chem. Soc.* **1999**, *121*, 7527; (e) Watanabe, M.; Nishiyama, M.; Yamamoto, T.; Koie, Y. *Tetrahedron Lett.* **2000**, *41*, 481; (f) Harris, M. C.; Buchwald, S. L. *J. Org. Chem.* **2000**, *65*, 5327; (g) Watanabe, M.; Yamamoto, T.; Nishiyama, M. *Chem. Commun.* **2000**, 133.
17. Anderson, J. D.; McDonald, E. M.; Lee, P. A.; Anderson, M. L.; Ritchie, E. L.; Hall, H. K.; Hopkins, T.; Mash, E. A.; Wang, J.; Padias, A.; Thayumanavan, S.; Barlow, S.; Marder, S. R.; Jabbour, G. E.; Shaheen, S.; Kippelen, B.; Peyghambarian, N.; Wightman, R. M.; Armstrong, N. R. *J. Am. Chem. Soc.* **1998**, *120*, 9646.
18. Shirota, Y. *J. Mater. Chem.* **2000**, *10*, 1.